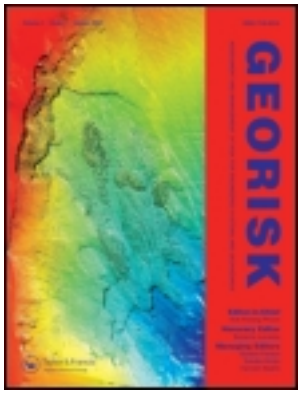

Georisk: Assessment and Management of Risk for Engineered Systems and Geohazards
Publication details, including instructions for authors and subscription information:
http://www.tandfonline.com/loi/ngrk20

Fragility curves in operational dike reliability assessment

D. Bachmann [a] , N.P. Huber [b] , G. Johann [c] & H. Schüttrumpf [a]

[a] Institute of Hydraulic Engineering and Water Resources Management, RWTH Aachen University, Aachen, Germany

[b] Bundesanstalt für Wasserbau W2 - Binnen, Kußmaulstraße 17, Karlsruhe, Germany

[c] Emschergenossenschaft/Lippeverband, Kronprinzenstraße 24, Essen, Germany

Version of record first published: 14 Feb 2013.

To cite this article: D. Bachmann , N.P. Huber , G. Johann & H. Schüttrumpf (2013): Fragility curves in operational dike reliability assessment, Georisk: Assessment and Management of Risk for Engineered Systems and Geohazards, 7:1, 49-60

To link to this article: http://dx.doi.org/10.1080/17499518.2013.767664

Georisk, 2013
Vol. 7, No. 1, 49–60, http://dx.doi.org/10.1080/17499518.2013.767664

Taylor & Francis
Taylor & Francis Group

Fragility curves in operational dike reliability assessment

D. Bachmann[a]*, N.P. Huber[b], G. Johann[c] and H. Schüttrumpf[a]

[a]*Institute of Hydraulic Engineering and Water Resources Management, RWTH Aachen University, Aachen, Germany;* [b]*Bundesanstalt für Wasserbau W2 – Binnen, Kußmaulstraße 17, Karlsruhe, Germany;* [c]*Emschergenossenschaft/Lippeverband, Kronprinzenstraße 24, Essen, Germany*

(Received 24 October 2012; final version received 14 January 2013)

Operational flood prediction and flood risk assessment have become important components of flood management. One main aspect is the reliability assessment of the flood defence line during a flood event. This is generally performed by a comparison of the water level in the river to the crest height of the dikes whilst taking only hydraulic and geometric aspects into account. Additional information about material zones and material parameters are often available. However, these data are not in an appropriate shape when deriving the reliability of the flood defence line. This paper outlines how the fragility curve of a dike section is used to appropriately integrate geostatic and geohydraulic dike characteristics into operational flood management systems. Fragility curves are the result of a model-based reliability analysis and they summarise the dike performance depending on the water level. Failure modes such as piping or slope failure are included. In a case study, fragility curves for dike sections along the River Emscher (Germany) are determined. Their practical implementation in an operational flood management system shows an improvement in the operational reliability assessment due to the additional information taken into account. The use of fragility curves also supports the decision-making processes when emergency flood protection measures are required.

Keywords: operational flood management; reliability analysis; dike failure; fragility curve

Introduction

Operational flood prediction and the assessment of flood safety have become important components of flood management. A primary aspect is the reliability assessment of the flood defence line during a flood event. These operational systems require fast access to easily interpretable flood management information.

Operational systems are important components of the flood management of the Emschergenossenschaft/Lippeverband (EGLV) (Grün and Johann 2012). The EGLV is responsible for the flood protection of an area covering approximately 4100 km^2 with approximately 3.7 million inhabitants. The EGLV manages 220 km of dikes which are mainly situated in the industrial region between Duisburg, Essen and Dortmund (Germany), as shown in Figure 1. As part of their operational flood management, EGLV has developed the dike data service system, termed D^3 (Grün and Johann 2012). The objective of the D^3 system is to support the early introduction of dike defence measures (see Figure 2).

One of the operational applications of the D^3 system is the assessment of dike reliability. This is currently assessed by comparing the existing or predicted water level to the crest height of the dike. However, the reliability of a dike depends not only on the hydraulic and geometric aspects but also on other aspects such as its geostatic and geohydraulic characteristics. Taking this into consideration offers a more realistic reliability assessment of flood defence structures, including their reliability during operation.

This paper focuses on the additional integration of geostatic and geohydraulic dike characteristics into an operational reliability assessment system, such as the D^3 system (see Figure 2), using fragility curves. Fragility curves show the probability of the failure of a structure as a function of the water level. They also summarise the geometrical as well as the geostatic and geohydraulic characteristics of a dike. The quick data access and simple interpretability that are required for an operational assessment are retained. To generate fragility curves, the reliability analysis of the modular program package ProMaIDes (Protection Measure against Inundation Decision Support) is applied (see Figure 2). One fragility curve of a selected cross section of the Emscher dike will be presented and further analysed. The practical integration of fragility curves of the Emscher River into the D^3 system as part of the EGLV's operational flood risk management will be ultimately discussed.

*Corresponding author. Email: bachmann@iww.rwth-aachen.de

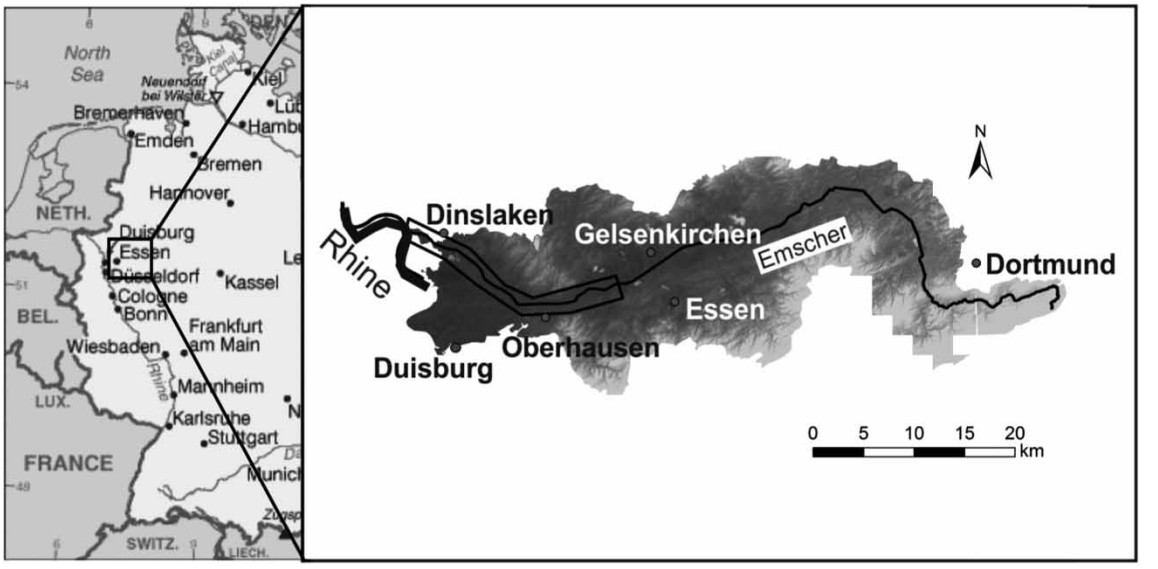

Figure 1. The Emscher area in Germany, course of the Emscher and location of the area under investigation (framed).

Fragility curves in strategic and operational flood management systems

The concept of the fragility curve was developed as part of the reliability analysis of engineering structures (e.g. Casciati and Faravelli 1991). According to Schultz et al. (2010), the application of fragility curves in flood management systems dates back to 1991 (USACE 1991), when the assessment of the economic benefit of flood protection was the main objective. Hall et al. (2003) and Dawson et al. (2005) integrated fragility curves into a national-scale flood risk assessment for the UK. Apel et al. (2004) used fragility curves for a flood risk assessment applied to a part of the River Rhine near Cologne (Germany).

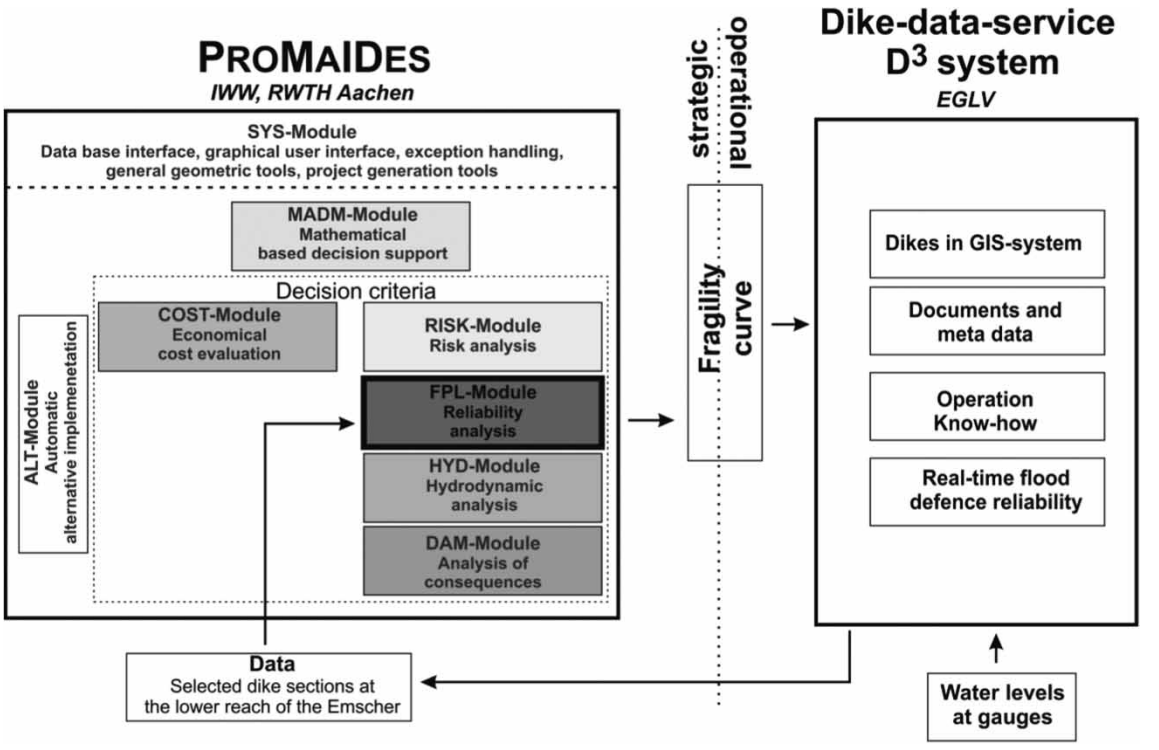

Figure 2. Structure of the decision support system ProMaIDes and the dike data service (D^3) system as well as the fragility curve as a data interface.

Further developments in the methods of determining fragility curves (e.g. Simm et al. 2009), the intrinsic level of detail (e.g. van der Meer et al. 2009) and their integration into flood risk assessment models (Vorogushyn et al. 2010; Bachmann 2012) have been researched and expanded since their conception. Various research projects concerning flood risk assessment have included the concept of the fragility curve (e.g. DEFRA/EA 2007; FLOOD*site* 2008; UrbanFlood 2011). Schultz et al. (2010) provide further information in a very detailed literature review about the development and application of fragility curves for flood protection measures in the last decade.

However, the application of fragility curves focuses mainly on the strategic flood risk assessment and the planning of flood protection measures. Trends show an increase in the application of fragility curves for assessing operational reliability, which is the main objective of this study (Schultz et al. 2010).

The dike data service (D^3) system

The D^3 system is operated by the EGLV to administrate the data required for the ongoing operation and maintenance of the dikes in the area monitored by the EGLV. The system is based on a flood defence line which is comprised not only of dikes but also of flood walls, inflows, bridges and the hinterland. Geometric information is available for 100-m sections of each dike section. The basic structure of the D^3 system is comprised of four elements (see Figure 2):

- Dikes in the geographical information system (GIS): Collection of design-relevant data for the dikes as well as the dikes' surroundings in a GIS which guarantees georeferencing of the available data.
- Documents and metadata: Metadata and dike-specific project works and reports, such as expert and dike reports, are managed using a document management system from the EGLV.
- Operation know-how: Operational data, observations and the resulting interpretations are collected in this expert application and made available for visualisation and further evaluation.
- Real-time flood defence reliability: The performance of the dikes along the rivers is evaluated by continuously comparing the crest height to flood water levels.

In addition to the static offline information regarding flood water design levels, the D^3 system also represents the current flood situation. Water levels based on 40 online connected gauging stations are transmitted every 15 minutes. The current flood levels are therefore determined along each dike sections.

Furthermore, the discharge forecasts (Johann, Ott, and Treis 2009) for the River Emscher (forecast timeframe: 6 h) and the River Lippe (forecast timeframe: 24 h) are linked to the D^3 system; the forecast discharges are converted into water levels at the dike sections, using water level–discharge relationships.

The decision support system: ProMaIDes

The modular-designed decision support system ProMaIDes (see Figure 2), which is being developed at the Institute of Hydraulic Engineering and Water Resources Management (RWTH Aachen University), is a tool for computer-based support in the selection of flood protection measures (Bachmann 2012; Huber et al. 2009). The effectiveness of a protective measure is evaluated using risk-based criteria. Additionally, the cost criteria (COST module) which evaluate the cost directly caused by the implementation of such a measure are taken into account. The integral risk is quantified mathematically using the general risk definition

$$R = \int K(x) \cdot f(x) dx \tag{1}$$

In Equation (1), R defines the integral risk, $f(x)$ the probability density function of the random variable X and $K(x)$ defines the consequences resulting from the realisation of random variable x (e.g. a flood event). The model-based flood risk analysis comprises three basic analyses (see Figure 2; the respective ProMaIDes modules are indicated in parentheses):

- Reliability analysis (FPL module): The probability of the failure of flood defence structures, such as dikes or flood walls, is quantified.
- Hydrodynamic analysis (HYD module): The flood event is transformed into hydraulic variables, such as water levels or flow velocities, taking into account the morphological characteristics of the river and the hinterland.
- Consequence analysis (DAM module): The hydraulic variables of a flood event across areas of specific land use are converted into consequences for the people, assets and goods located in these affected areas of the hinterland.

The task of the risk analysis (RISK module) is to combine the results of the named basic analyses into

an integrated flood risk (see Equation (1)) for the analysed system.

In order to effectively support the design and selection of flood protection measures, the ProMaIDes software package is supplemented with a graphical user interface and a database interface besides the mathematical algorithms which prioritise flood protection measures, based on multiple attribute decision methods (MADM module).

With the decision support system ProMaIDes that can support the tasks relating to §73 'Evaluation of flood risk', §74 'Hazard maps and risk maps' and §75 'Risk management plans' of the German Federal Water Act based on the EU-Flood Directive 2007 (Wasserhaushaltsgesetz; BMU WHG 2009), detailed information about the ProMaIDes decision support system and the theoretical fundamentals of procedure implementation are provided by Bachmann (2012).

To calculate fragility curves as an interface of the EGLV's D^3 system, only the reliability analysis (FPL module) is used.

Theoretical background of reliability analysis

General

The objective of reliability analysis is to quantify the probability of a failure event for a structure. The probability of the complementary event (non-failure event) describes the reliability of a structure.

In principle, three approaches are used to determine the probability of failure (see Figure 3), as proposed by DEFRA/EA (2007):

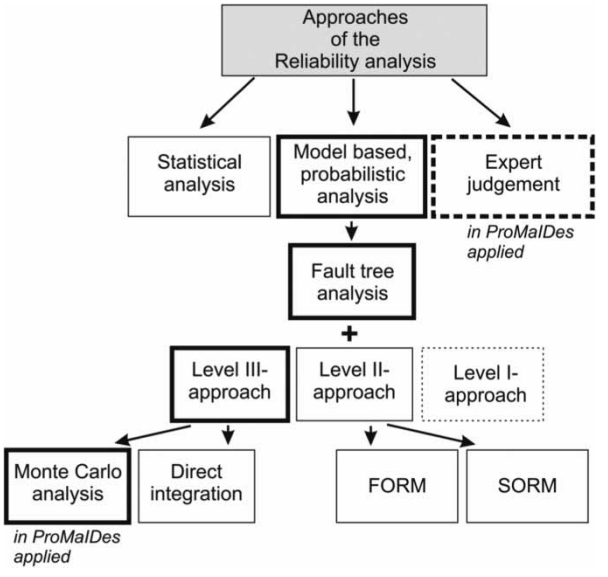

Figure 3. Categorisation of approaches for determining the probability of failure: detailed division of the approaches for model-based probabilistic analysis.

- Statistical analysis based on observations or measurements of the event
- Model-based probabilistic analysis
- Expert judgement

A hybrid application of the above-mentioned approaches is possible (Schultz et al. 2010). For linear flood defences, the application of statistical analysis proved to be limited due to the amount of data available.

The expert judgement procedure is based on the assessment of structural reliability by experts who have experience with this type of structure and the appropriate professional qualifications. This approach is used only in cases where no data or model procedures are available (Merz 2006).

The model-based probabilistic analysis can be divided into three essential stages. The first step is the configuration of a deterministic model, derived from a system analysis of the structure. Therefore, a structured evaluation of the events leading to failure and the interaction between these events is required. The fault tree analysis (Hartford and Baecher 2004) is an established tool used to support this step.

The processes that lead to a failure event are modelled based on physical or empirical principles. These processes result in the failure mechanisms of the system. In general, the failure mechanisms are mathematically formulated using the limit state function $Z(R, S)$. This compares the stress S on a structure with the resistance R:

$$Z(R, S) = R - S \tag{2}$$

If the stress S is greater than the resistance R, whereby $Z(R, S)$ is less than zero, then the structure will fail. The input variables determining the stress are loading variables, such as water levels or wind speeds. The resistance-relevant variables are geometric and material-specific characteristics of the structure.

In the second step, the statistical description of the input variables is selected based on available data or expert knowledge. They are characterised by their mean values, standard deviations and distribution types taking into account natural variability (aleatoric) and epistemic uncertainties.

The last step in a model-based probabilistic analysis calculates the propagation of the probability distributions of the input variables to the probability of occurrence of the defined failure event (Merz 2006). Monte Carlo analysis is used within the FPL module of the decision support system ProMaIDes, as a Level III procedure (CUR 141 1990). It is robust and can model even complex fault tree models which

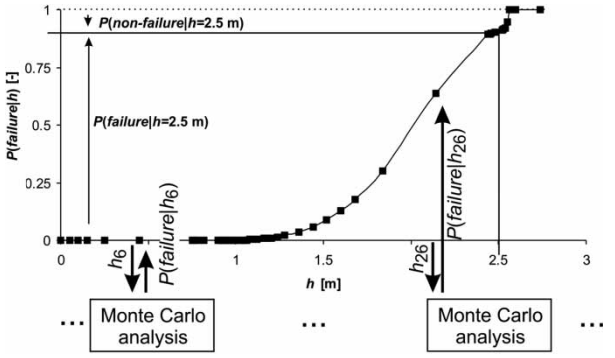

Figure 4. Determination of the conditional probability of failure $P(\text{failure}|h)$ via the fragility curve $Frc(h)$; calculation of discrete nodes of the fragility curve via the Monte Carlo analysis.

include complex failure mechanisms without simplifications or approximations.

Theory of the fragility curve

The fragility curve $Frc(h)$ expresses the reliability of a structure as a function of a defined dominant stress variable (Hall et al. 2003). In this context, the water level at the structure is defined as the dominant stress variable. The curve shows the conditional probability of the occurrence of a failure event $P(\text{failure}|h)$ [-] on the vertical axis as a function of the water level h [m], represented on the horizontal axis (see Figure 4).

The conditional probability of occurrence of a non-failure event (complementary event) is calculated using

$$P(\text{non} - \text{failure}|h) = 1 - P(\text{failure}|h) \qquad (3)$$

The fragility curve starts at the origin – a stress of zero results in a probability of failure of zero – and gets closer to one as the stresses increase. For common failure mechanisms, the curve rises monotonically.

For complex limit state functions and integrated modelling of the dependency of the failure mechanism within a fault tree analysis, a closed analytical derivation of a fragility curve is not feasible. Therefore, the fragility curve is derived numerically by calculating discrete nodes (Bachmann, Huber and Schüttrumpf 2009). Each Monte Carlo analysis calculates one discrete node of the fragility curve, whereas the water level at the structure h_i [m] is modelled as a deterministic variable. The result of the Monte Carlo analysis is the conditional probability of failure at this water level: $P(\text{failure}|h_i)$ [-] (see Figure 4).

Processes, failure mechanisms and fault tree analysis of a dike

The model set-up represents an essential work step in the model-based probabilistic reliability analysis. The processes and failure mechanisms of a dike, as considered in ProMaIDes, are summarised in Figure 5. The links between the events, which lead to the main event – a failure event of the structure – are represented in the type-specific fault tree. All mechanisms are modelled as steady-state processes, which gives a conservative upper bound on the probability of failure.

The failure mechanisms are subdivided into three categories: hydraulic, geohydraulic and geostatic. The hydraulic and geostatic events are individual events

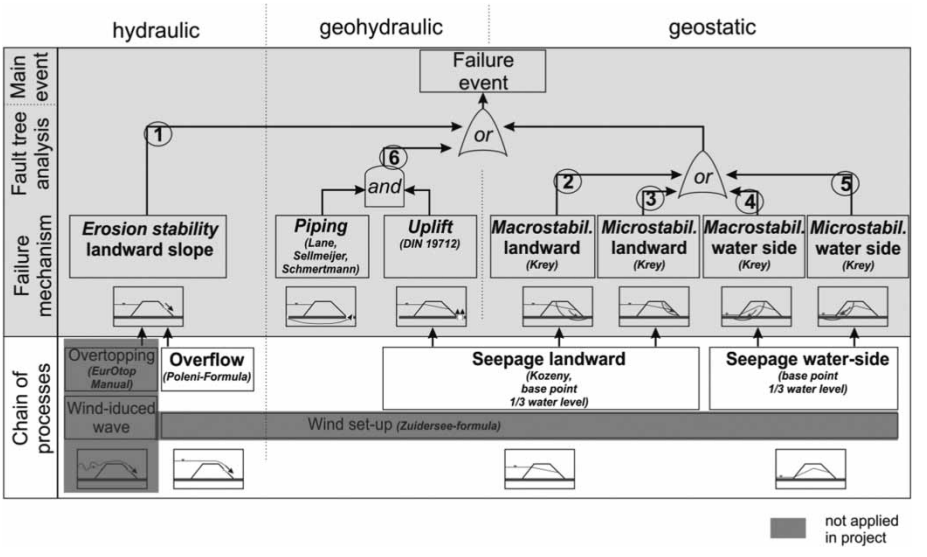

Figure 5. Fault tree analysis, failure mechanisms, process chains and the hierarchical order of failure mechanisms (numbers) of a dike implemented in ProMaIDes.

which lead directly to failure. They are combined via the '*or* operator' in the fault tree, indicating serial system behaviour.

In the hydraulic category, the failure mechanism of the erosion stability of the landward dike slope is taken into consideration. Triggering events can be overflow (POLENI-formula) or overtopping (Pullen et al. 2007) due to wind-induced waves.

For geostatic failure events, the stability of the landward and the water side slopes are analysed with the segment-based method according to Krey (e.g. DIN 4084 2009) calculating slip circles. These events are further divided into macro- and microstability. Using a raster-based search for the centre and the radius of the critical slip circle a problem arises, where critical slip circles are found and which include only a very small area of the dike body. A total failure of the dike is not plausible. Therefore, additional assumptions are made, besides the limit state function which includes stress and resistance momenta (see Equation (2)). A macrostability failure occurs if more than half of the dike crest is included in the slip circle. A large volume of the dike body is lost due to the sliding, and total failure is therefore assumed. In contrast to macrostability is the additional condition of a microstability failure which does not depend on the area of the slip circle. In this case, an intersection with the seepage line is required. It is assumed that the material of the dike body is eroded away by seepage water which leads to failure.

In the geohydraulic category, an uplift event (DIN 19712 1997) must take place in combination with a piping event for failure to occur. To model the piping process, three different approaches are implemented and compared: Lane (1935), Sellmeijer (1988) and Schmertmann (2000). The required combined occurrence of the events of uplift and piping is represented by the '*and* operator' in the fault tree, indicating a parallel system behaviour. This combined event leads to a failure event and is linked to the previously mentioned hydraulic and geostatic events via an '*or* operator'.

The dark grey-shaded processes and failure mechanisms shown in Figure 5 are implemented in the reliability analysis of PROMAIDES, but are not applied within the presented study. They relate to the process of overtopping triggered by wind-induced waves and the process of wind set-up, which are neglected due to the short fetch length (maximum 50 m) in the area under investigation.

A hierarchical order of failure mechanisms is specified by the numbering in Figure 5. This order does not affect the determination of the total fragility curve. It is necessary to determine partial fragility curves for the failure mechanisms which are combined as a serial system in the fault tree. They indicate the contribution of each failure mechanism to total failure by taking their dependency into account. The superposition of each partial fragility curve results in the fragility curve of total failure. The shape of the total fragility curve gets traceable (see *Results* section). The order is proposed based on the assumed rate of degradation of the dike performance per mechanism.

The segregated fragility curve, which is also a result of the Monte Carlo analysis, provides further information about the performance of the analysed dike section. It shows the conditional probability of the occurrence of an event $P(\text{event}|h)$ [-] on the axis of abscissa as a function of the water level h [m], represented on the axis of ordinates. In contrast to the total fragility curve and the partial fragility curve where the event is defined as failure, in this case the definition of an event is more general; the occurrence of an uplift event which does not lead directly to failure or the exceedance of a stated wave height can be defined as an event. No dependencies due to same input variables between the mechanisms are taken into account. Each mechanism modelled as a serial system is regarded separately, whereas a superposition is not valid. The segregated fragility curves provide information about the weak part of the dike, for example the underground, body or slope, what supports the derivation of effective emergency or reinforcement measures (see *Results* section)

Determination of fragility curves for the lower reach of the Emscher

The model area

The Emscher rises to the south-east of Dortmund, flows through the industrial region between Essen and Duisburg (Germany) and discharges into the Rhine after approximately 85 km near Dinslaken (see Figure 1). Its catchment area measures approximately 865 km^2. In total, there are 75 km of dikes along the main course of the Emscher (EGLV 2011).

The reliability analyses performed are limited to a region of approximately 25 km in length along the Emscher. It starts from the mouth of the Emscher and ends upstream in the area between Oberhausen and Essen (see Figure 1).

The dike bodies are composed of sand materials of various bulk densities or washed rock material (excavation material from the coal mining industry). A combination of these materials is possible. No drainage filters or impermeable cores exist. The average embankment slope on the water and the landward side is approximately 1:2, which is relatively

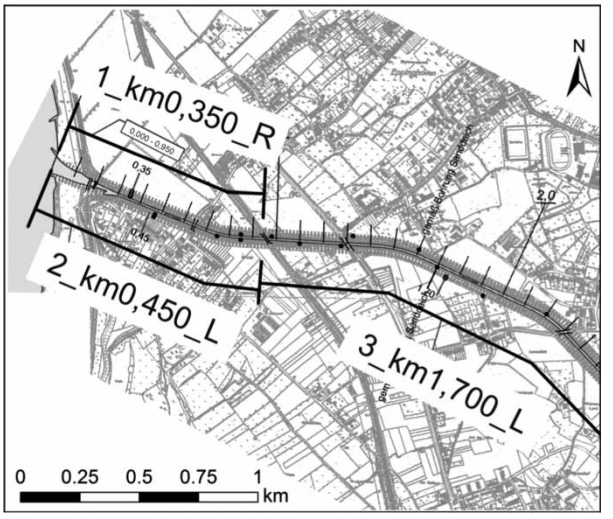

Figure 6. Area of influence of the dike cross sections as a dike section with quasi-homogenous characteristics for dike sections 1, 2 and 3.

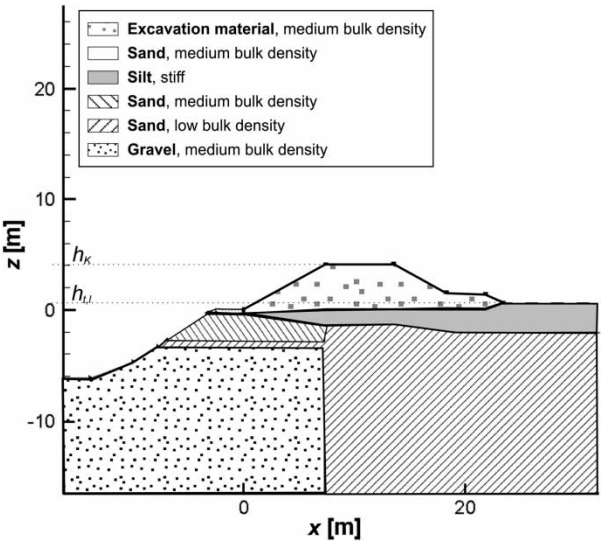

Figure 7. Cubature and geometric parameterisation by material zone of dike cross section 2 (the bold-plotted material specifications correspond to Table 1).

steep in comparison with the recommendations given by DIN 19712 (1997), which proposes a slope of 1:3. The dikes are partially built on a less permeable blanket layer of clay or silt. Beneath this covering layer, permeable sand layers are found.

Input data of the dike sections

In total, fragility curves for 33 dike cross sections are calculated along the Emscher which represent predefined dike sections. The sections length varies from 500 to 1500 m. The assumption is that the dike characteristics and the dike geometry in these sections are quasi-homogenous and can be represented in the model with sufficient accuracy using the parameterised cross section.

Figure 6 shows the extent of the dike sections 1, 2 and 3 situated near to the mouth of the Emscher.

The geometric parameterisation of the dike cubature and the material zones was performed using geometric data available from the EGLV. Figure 7 shows the geometric parameterisation of dike cross section 2 on the left bank of the Emscher (see Figure 6). The dike section extends over 950 m. This cross section is discretised by six material zones with different material properties. The dike body comprises excavation material of medium density, whilst the underlying covering layer is comprised of silt. The permeable layers beneath the covering layer are primarily characterised by sand and gravel. The crest height h_K [m] on the water side dike toe is approximately 4.0 m, and the height of the landward dike toe $h_{t,l}$ [m] is about 0.6 m above the water side dike toe.

The parametric characteristics of material-specific properties required for a probabilistic analysis are the mean value and the standard deviation. The mean values for the angle of friction, cohesion or density are based on existing data sets. They have been verified and supplemented using published values. A data-set to determine the standard deviations of material-specific characteristics does not exist. Therefore, published values were summarised and applied (Huber 2008; Baecher and Christian 2003). As an example, Table 1 summarises the available and applied values of the variation coefficient of the angle of friction for different soil materials as layer averaged values.

Results

The following conditions were applied to calculate the fragility curves:

- For each Monte Carlo simulation (the calculation of the probability of failure depending on one deterministic water level) a maximum of 50,000 and a minimum of 5000 Monte Carlo runs are performed. The 95% confidence interval between the 5% and the 95% quantile calculated after Haugh (2004) is about 7.0×10^{-3}.
- Depending on the dike cross section, approximately 60–130 Monte Carlo simulations are performed in order to determine a discrete fragility curve.

- In total, 300–800 slip circles per dike cross section (landward/water side) are analysed, which gives sufficient confidence in finding the critical slip circle.

Table 1. Variation coefficient of the angle of friction for different soil materials.

Soil material	Baecher and Christian (2003)	CUR 141 (1990)	Phoon and Kulhawy (1999)	Applied value
Clay	0.12–0.56	0.20	0.03–0.56	0.20
Silt	–	–	–	0.20
Sand–silt mix	–	0.05–0.508	–	0.30
Sand	0.05–0.15	0.10	0.05–0.14	0.08
Gravel	–	–	–	0.10
Excavation material	–	–	–	0.09

Under these conditions and using an Intel(*R*) Core™2 Quad CPU with 2.50 GHz, the calculation takes 4–20 hours per dike cross section.

Figure 8 presents the total fragility curves of dike section 2 by modelling the piping mechanisms using three different approaches. Quantitative information about the dike reliability becomes accessible, even when the water level is below the crest height h_K. An analysis of the partial and the segregated fragility curves provides further information.

The partial fragility curves of the individual failure mechanisms, which are modelled in the fault tree using a hierarchical order of the failure mechanisms (see Figure 5) are shown in Figure 9. The failure mechanisms include macro- and microstability on the landward and water side (whereby in this case only the microstability on the water side contributes to the total fragility curve), the piping mechanism modelled by three different approaches and the mechanism of erosion stability of the landward embankment. The microstability on the water side is influenced by an assumed linear decreasing seepage line from the modelled peak water level h in the middle of the dike to the water side dike toe. A superposition of the partial fragility curves results in the total fragility curves shown in Figure 8.

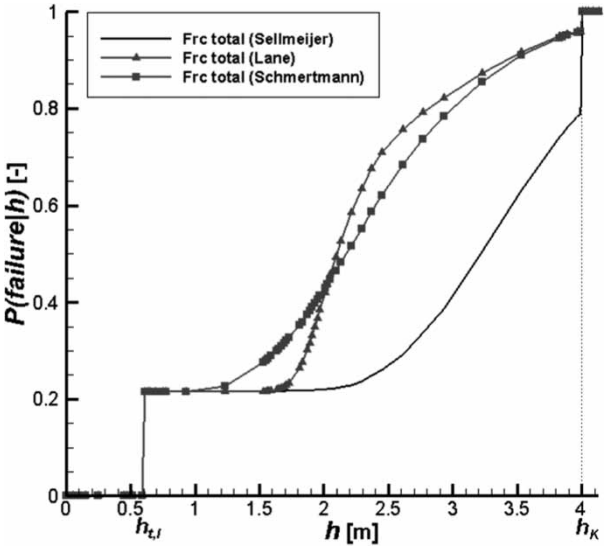

Figure 8. Total fragility curve for dike section 2; the piping mechanism is modelled by three different approaches represented by three different fragility curves.

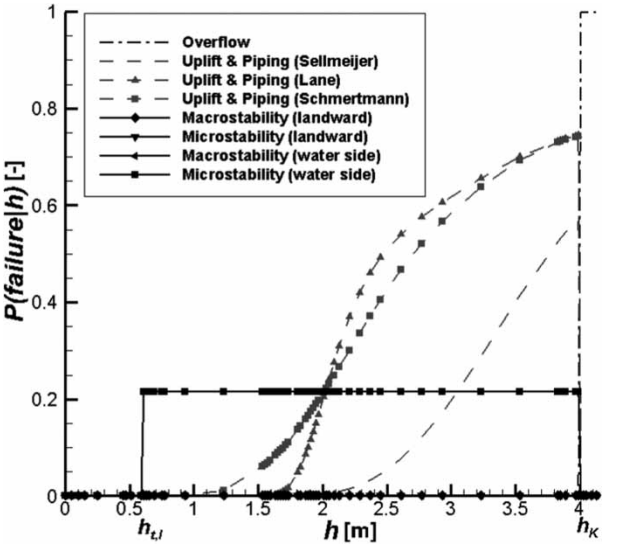

Figure 9. Contribution of the individual failure mechanisms to the total fragility curve represented by the partial fragility curves for dike section 2.

The influence of the individual failure mechanism reduces in accordance with the hierarchical order. The hierarchical order becomes particularly evident when the water level h exceeds the dike crest height h_K. The failure mechanism of the erosion stability of the landward embankment, which is first in the hierarchical order, is solely responsible for a failure event. The contribution of all other failure mechanisms is in model-based calculation zero; they become irrelevant.

The total fragility curve is partly discontinuous (see Figure 8). An analysis of the partial fragility curves (see Figure 9) indicates that:

- The landward dike toe ($h_{t,l}$ about 0.6 m) is above the water side dike toe (0.0 m). By definition, the occurrence of a failure event is only possible, if the water level h exceeds the landward dike toe. Therefore, the failure event

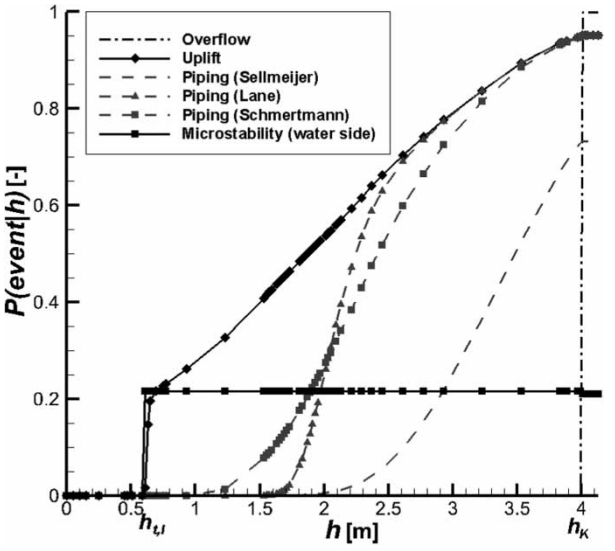

Figure 10. Segregated fragility curves of mechanisms for dike section 2, neglecting the dependencies of the events.

of microstability occurs abruptly by exceeding the landward dike toe. It is expressed by a vertical jump of the fragility curve.

- Failure events occur suddenly when a certain water level is reached; if the water level h exceeds the crest height h_K in combination with a low resistance of the landward embankment with respect to an overflow event, then the fragility curve takes a vertical step.

The shape of the total fragility curve (see Figure 9) for low water levels (up to $h = 1.0$ m) is entirely affected by a failure event of microstability of the water side. A horizontal gradient shows the independence of the water level and the probability of failure. It is caused by a water saturated critical slip circle lying near the water side dike toe. A rising water level has no more relevant influence to the stability. A further increase of the total fragility curve at about $h = 1.0$ m / 1.5 m / 2.0 m (Schmertmann/Lane/Sellmeijer) is the result of an increasing probability of failure due to piping until the crest height is reached.

For the applied data-set, the application of the Lane and Schmertmann methods resulted in very similar fragility curves. The Sellmeijer method models a higher resistance of the dike against piping failure. Sellmeijer (1988) stated similar results and suggested a deterministic safety factor of 1.5–2.5 to adapt the results of the Sellmeijer approach to the conservative results of the Lane approach. The shape and inclination of the fragility curve using the Sellmeijer and Schmertmann approaches are very similar, but have different starting points. This supports the idea of an intrinsic deterministic factor.

The fragility curves calculated using Sellmeijer's piping approach are recommended for transferral into the EGLV's D^3 system. The reasons for recommending the Sellmeijer approach are thus; first, in contrast to the Lane approach, it includes more input variables which enable the area under investigation to be modelled in more detail. Second, it is successfully applied and validated for several years in different applications, whereas the Schmertmann approach is not commonly used. Third, a deterministic safety factor disagrees with a more progressive probabilistic reliability assessment.

A comparison of the partial fragility curves (see Figure 9) to the segregated fragility curves (see Figure 10) illustrates their differences. For low water levels ($h < 2.5$ m), the curves representing the piping mechanism are very similar, which means that the dependency on the microstability event on the water side is negligible. For higher water levels, higher probabilities of occurrence are calculated, so the dependency is no longer negligible. A superposition of the segregated fragility curves is no longer feasible.

An analysis of the segregated fragility curves of uplift and the piping mechanisms indicates that an occurrence of an uplift event is very probable even at low water levels ($h < 2$ m). Not every event results in a total failure because of the modelled parallel system behaviour to the piping mechanism. For higher water levels ($h > 2$ m) using the Lane or Schmertmann piping approach, every uplift event results in a piping failure.

Upon interpretation of the partial and segregated fragility curves, it becomes obvious that planned measures (e.g. relief ditch) or emergency triggered measures (e.g. sand bags) against uplift could essentially improve the dike performance of dike section 2. A planned flattening of the slope near the water side dike toe could further increase the dike performance by reducing the probability of failure due to water side instability.

Extension of the D^3 system using fragility curves

The principle of using fragility curves within the D^3 system is summarised as follows (see Figure 11). The generated fragility curves of the lower reach of the River Emscher are linked to the D^3 system using the water level information. A real-time assessment of the reliability of the dike sections which takes geostatic and geohydraulic aspects into account therefore becomes feasible. In analogy to the currently used representation of their reliability, which is based upon a comparison of water level and crest

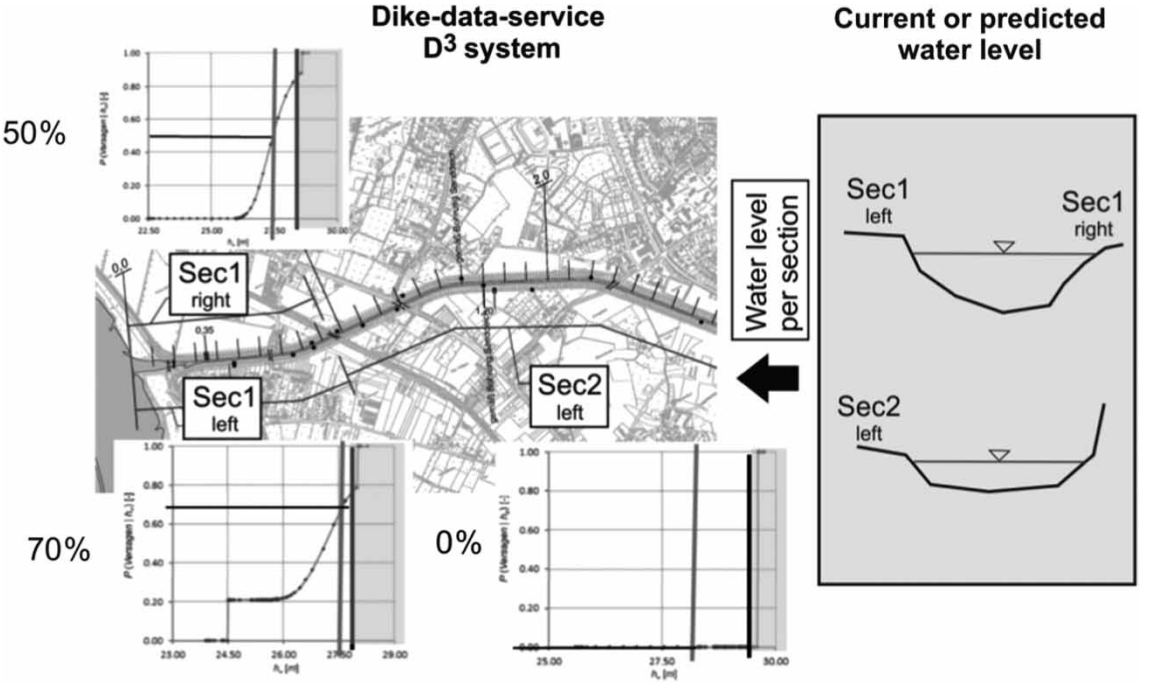

Figure 11. Sample illustration of the operational assessment of dike reliability depending on fragility curves and water level in the D^3 system per dike section.

height, the dike sections are represented in different colours depending on their reliability and the current or predicted water level. This means that the dike sections can be assessed quickly whilst in operational use.

Practical operational flood management based on fragility curves

The practical decision-making within an operational flood management system raises one main challenge once the model-based character of the results with all the associated assumptions and simplifications are taken into account: finding the adequate action to take, if a certain probability of failure is reached.

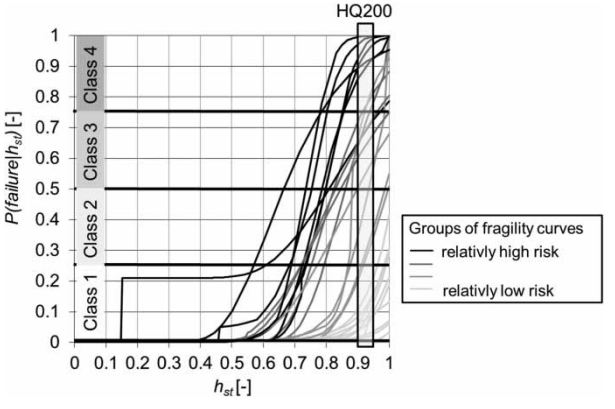

Figure 12. Comparison of the geostatic and geohydraulic dike performance using a standardised water level h_{st} related to the crest height h_K.

To get an overview of the geostatic and geohydraulic performance of each calculated dike section, all the fragility curves were made to be comparable. To guarantee comparability of the dike sections, the water level h_j was standardised by division of the crest height $h_{K,j}$ per dike section j (see Figure 12). A standardised water level h_{st} [-] between 0.90 and 0.95 corresponds to the water level in the dike section due to a 200-year flood event (HQ200, design discharge).

The fragility curve of the dike sections can be qualitatively clustered into four groups. The groups differ in terms of starting point and gradient of the fragility curve.

A classification of the probability of failure was performed by expert judgement supported by the clustering shown in Figure 12. It was coordinated with the EGLV's 'Operations' department, which uses the D^3 system when responding to flooding. It initiates dike defence measures and implements them. Personnel deployments are also planned on the basis of the information in the D^3 system.

In the first step, an equidistant division of the probability of failure into four classes is proposed (see Figure 12). A precise statement for triggering any flood defence measure can only be given for the first class. For the lowest probability of failure class (no significant loading of the dike), no measure has to be

triggered. For the other classes, increasing intervals of observation for the concerned dike section are preliminarily proposed. Whether this classification will be effective in practice is yet to be seen in flood exercises or in the event of an actual flood. An adaption of classes and corresponding measures will be checked at this stage.

The standardised fragility curves shown in Figure 12 make an assessment of the occurrence probability of each class feasible for each dike section. For example, 6–10 dike sections will meet the highest probability of failure class (class 4) in case of an HQ200 flood event.

In a strategic flood management evaluation, the standardised fragility curves indicate which dike section represents the highest probability of failure in case of flood event. With this knowledge, flood responses can be planned more effectively before the event and additional dike-strengthening measures can be executed.

Conclusion

Within this study, probabilistic based results were generated in the form of fragility curves using existing dike data about material zones and parameters. The assessment of the reliability includes geostatic and geohydraulic aspects and is not restricted to a pure comparison of the crest height of the dike and the existing river water level. An extended reliability assessment of dikes which retains quick access and simple interpretability of the relevant information is achieved using fragility curves as the data interface of an operational system such as the EGLV's D^3 system.

The generation of fragility curves for 33 selected dike cross sections on the lower reach of the Emscher was performed using the reliability module of the software package ProMaIDes which is being developed at the Institute of Hydraulic Engineering and Water Resources Management (RWTH Aachen University). The implemented fault tree model for dikes includes hydraulic, geostatic and geohydraulic failure mechanisms. A Monte Carlo analysis applied to the fault tree model integrates the distribution density functions of the input parameters into a failure probability. The inherent uncertainties of the model could be reduced by a further improvement of this implementation, for example by integrating additional failure mechanism or time-dependent processes. This would further enhance the quality and validity of the resulting fragility curves.

The practical application of fragility curves as a basis for decision-making in an operational flood management system requires a sensible handling when taking the model-based character of the results into account. At this stage of the implementation process, a classification into four equidistant classes is used, depending on the level of probability of failure. According to these classes, observation intervals of the vulnerable dike sections are increasingly exposed. A permanent inquiry and improvement of the classes and the corresponding defence measures are required. In the near future, fragility curves for dike sections of the upper reach of the Emscher will be calculated to achieve a full covering of the area managed by the EGLV.

References

Apel, H., A. H. Thieken, B. Merz, and G. Bloschl. 2004. "Flood Risk Assessment and Associated Uncertainty." *Natural Hazards and Earth System Science* 4: 295–308. doi:10.5194/nhess-4-295-2004.

Bachmann, D. 2012. "Beitrag zur Entwicklung eines Entscheidungsunterstützungssystems zur Bewertung und Planung von Hochwasserschutzmaßnahmen [Development of a decision support system for the assessment and design of flood mitigation measures]." PhD diss., Institut für Wasserbau und Wasserwirtschaft, RWTH Aachen; http://darwin.bth.rwth-aachen.de/opus3/volltexte/2012/4043.

Bachmann, D., N. P. Huber, and H. Schüttrumpf. 2009. "Fragility Curve Calculation for Technical Flood Protection Measures by the Monte Carlo Analysis." In *Flood Risk Management: Research and Practice*, edited by P. Samuels et al., 677–685. London: Taylor & Francis.

Baecher, B. B., and J. T. Christian. 2003. *Reliability and Statistics in Geotechnical Engineering*. West Sussex: John Wiley & Sons.

BMU WHG. 2009. "Gesetz zur Ordnung des Wasserhaushalts [German Federal Water Act]." Wasserhaushaltsgesetz – WHG. Accessed June 9. http://www.bundesrecht.juris.de/bundesrecht/whg_2009/gesamt.pdf.

Casciati, F., and L. Faravelli. 1991. *Fragility Analysis of Complex Structural Systems*. West Sussex: John Wiley & Sons Inc.

CUR 141, 1990. *Probabilistic Design of Flood Defences*. Gouda (NL): Stichting Civieltechnisch Centrum Uitvoering Research en Regelgeving.

Dawson, R., J. Hall, P. Sayers, P. D. Bates, and C. Rosu. 2005. "Sampling-based Flood Risk Analysis for Fluvial Dike Systems." *Stochastic Environmental Research and Risk Assessment* 19: 388–402. doi:10.1007/s00477-005-0010-9.

DEFRA/EA, 2007. *R&D Technical Report FD2318/TR1 – Performance and Reliability of Flood and Coastal Defences*. Vol. 1. London: DEFRA/EA Joint R&D FCERM Programme.

DIN 19712, 1997. *Flußdeiche* [River Dikes]. Berlin: Beuth Verlag GmbH.

DIN 4084, 2009. *Baugrund –Geländebruchberechnung* [Analysis of base and slope failure]. Berlin: Beuth Verlag GmbH.

EGLV, 2011. "Emscher in Zahlen; Emschergenossenschaft/ Lippeverband [Data of the emscher river]". Accessed April 6. http://www.eglv.de/emschergenossenschaft/emscher/zahlen-und-daten.html.

FLOOD*site*, 2008. Reliability Analysis of Flood Sea Defence Structures and Systems (Main Text); Report Number T07-08-01. Accessed December 3. http://www.floodsite.net/html/partner_area/project_docs/T07_08_01_Reliability_Analysis_D7_1_v2_1_P01.pdf.

Grün, E., and G. Johann. 2012. "Hochwassermanagement im urbanen Umfeld [Flood Risk Management for Urban Areas]." In *Hochwasserschutz - eine Daueraufgabe: 42.Internationales Wasserbausymposium, Aachen (IWASA)*, edited by H. Schüttrumpf. Aachen: Shaker. http://www.iww.rwth-aachen.de/de/menue/iwasa/iwasa2012.html.

Hall, J., R. Dawson, P. Sayers, C. Rosu, J. U. Chatterton, and R. Deakin. 2003. "A Methodology for National-scale Flood Risk Assessment." *Water & Maritime Engineering* 156 (WM3): 235–247. doi:10.1680/wame.2003.156.3.235.

Hartford, D. N. N., and G. B. Baecher. 2004. *Risk and Uncertainty in Dam Safety*. London: Thomas Telford Ltd.

Haugh, M. 2004. *Output Analysis and Run-length Control*. Accessed December 12. http://www.columbia.edu/ ~ mh2078/MCS04.html.

Huber, N. P. 2008. "Probabilistische Modellierung von Versagensprozessen bei Staudämmen [Probabilistic modelling of failure processes of embankment dams]." PhD diss., Institut für Wasserbau und Wasserwirtschaft, RWTH Aachen.

Huber, N. P., D. Bachmann, U. Petry, J. Bless, O. Arránz-Becker, A. Altepost, M. Kufeld, et al., 2009. "Ein Konzept für eine risikobasierte Entscheidungshilfe im Zuge der Identifikation von Schutzmaßnahmen bei extremen Hochwasserereignissen [Approach for risk based decision support system to identify flood protection measures]." *Hydrologie und Wasserbewirtschaftung* 53 (3): 154–159.

Johann, G., B. Ott, and A. Treis. 2009. "Einfluss von terrestrisch gemessenen und radarbasierten Niederschlagsdaten auf die Qualität der Hochwasservorhersage [Influence of terrestrial measured and radar based rainfall data to the quality of flood prediction]." *Korrespondenz Wasserwirtschaft* 2 (9): 487–493.

Lane, E. W. 1935. "Security from Under-Seepage-Masonry Dams on Earth Foundations." *Transaction American Society of Civil Engineering* 100: 1235–1351. http://cedb.asce.org/cgi/WWWdisplay.cgi?277074.

Merz, B. 2006. *Hochwasserrisiken - Grenzen und Möglichkeiten der Risikoabschätzung* [Flood risk and flood risk assessment]. Stuttgart: Schweizerbart'sche Verlagsbuchhandlung.

Phoon, K. -K., and F. H. Kulhawy. 1999. "Characterization of Geotechnical Variability." *Canadian Geotechnical Journal* 36 (4): 612–624. doi:10.1139/t99-038.

Pullen, T., N. H. W. Allsop, T. Bruce, A. Kortenhaus, H. Schüttrumpf, and J. W. van der Meer. 2007. *Die Küste: EurOtop Wave Overtopping of Sea Defences and Related Structures Assessment Manual*. Heide i. Holstein: Kommissionsverlag: Boyens Medien GmbH.

Schmertmann, J. H. 2000. "The No-Filter Factor of Safety Against Piping Through Sands." In *Judgement and Innovation: The Heritage and Future of the Geotechnical Engineering Profession,* vol.111, edited by F. Silva, et al., 65–133. Reston, VA: American Society of Civil Engineers.

Schultz, M., B. Gouldby, J. Simm, and J. Wibowo. 2010. *Beyond the Factor of Safety: Developing Fragility Curves to Characterize System Reliability*. Washington, DC: ERDC SR 10 1. G. a. S. Laboratory, USACE.

Sellmeijer, J. B. 1988. "On the Mechanism of Piping under Impervious Structures." PhD diss., Delft Geotechnics.

Simm, J., B. Gouldby, P. Sayers, J.-J. Flikweert, S. Wersching, and M. Bramley. 2009. "Representing Fragility of Flood and Coastal Defences: Getting Into the Detail." In *Flood Risk Management: Research and Practice*, edited by P. Samuels et al., 621–631. London (UK): Taylor & Francis.

UrbanFlood. 2011. The design and prototyping of a decision support system for flood control; Work Package 4-D4.1. Accessed December 3. http://www.urbanflood.eu/Pages/Deliverables.aspx.

USACE. 1991. Benefit determination involving existing levees. Policy Guidance Letter 26, Memorandum for Major Subordinate Commands and District Commands, Washington DC.

van der Meer, J. W., W. L. A. ter Horst, and E. H. van Velzen. 2009. "Calculation of Fragility Curves for Flood Defence Assets." In *Flood Risk Management: Research and Practice* edited by P. Samuels et al., 567–573. London: Taylor & Francis.

Vorogushyn, S., B. Merz, K.-E. Lindenschmidt, and H. Apel. 2010. "A New Methodology for Flood Hazard Assessment Considering Dike Breaches." *Water Resources Research* 46: 17. doi:10.1029/2009WR008475.